Support Information for

A Robust Indium-Porphyrin Framework for CO_2 Capture and Chemical Transformation

Lei Xu,[a] Meng-Ke Zhai,[a] Xin-Chao Lu,[a] Hong-Bin Du[a*]

[a] State Key Laboratory of Coordination Chemistry, Collaborative Innovation Center of Chemistry for Life Sciences, School of Chemistry and Chemical Engineering, Nanjing University, Nanjing, 210023, China. E-mail: hbdu@nju.edu.cn

Table of Contents

S1. Optical and SEM images of the obtained NUPF-3 crystals.

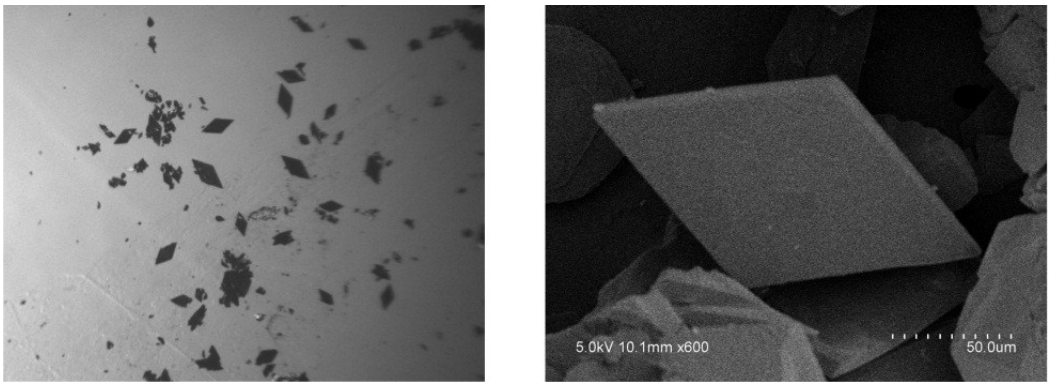

Fig. S1 Optical and SEM images of the obtained NUPF-3 crystals.

S2. PXRD pattern of as-synthesized NUPF-3.

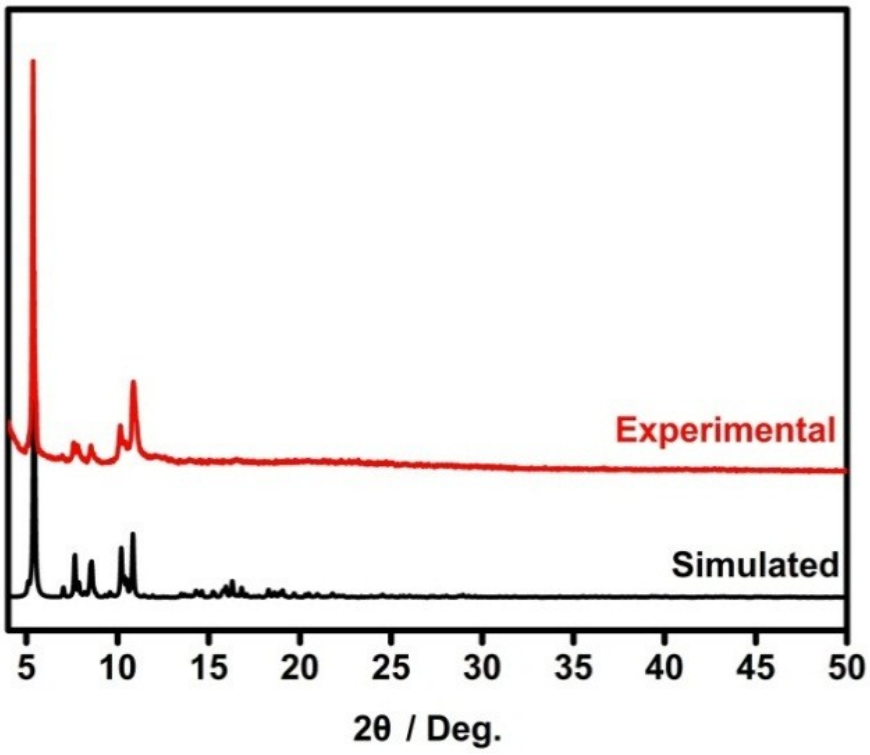

Fig. S2 PXRD patterns of NUPF-3.

S3. FT-IR spectra of NUPF-3.

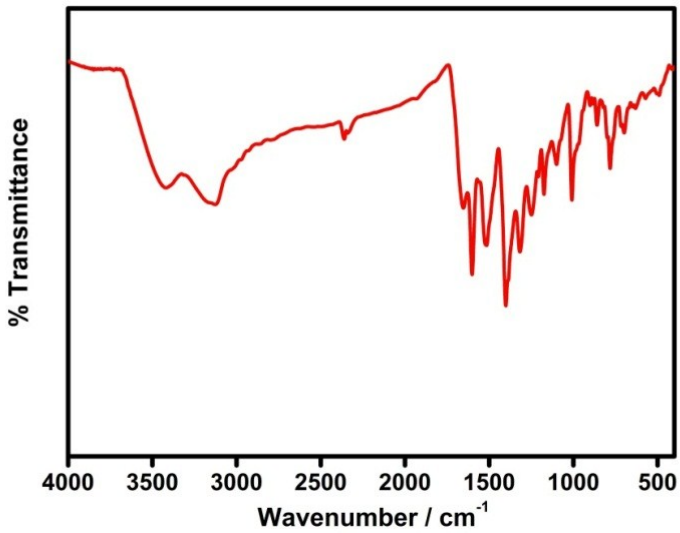

Fig. S3 FT-IR spectra of NUPF-3 measured at room-temperature.

S4. Solid-state UV-Vis spectra of NUPF-3.

As shown in Fig. S4, the band at 390 nm was attributed to the S band of porphyrin ligands in NUPF-3. The bands at *ca.* 508 and 590 nm were ascribed to the Q bands.

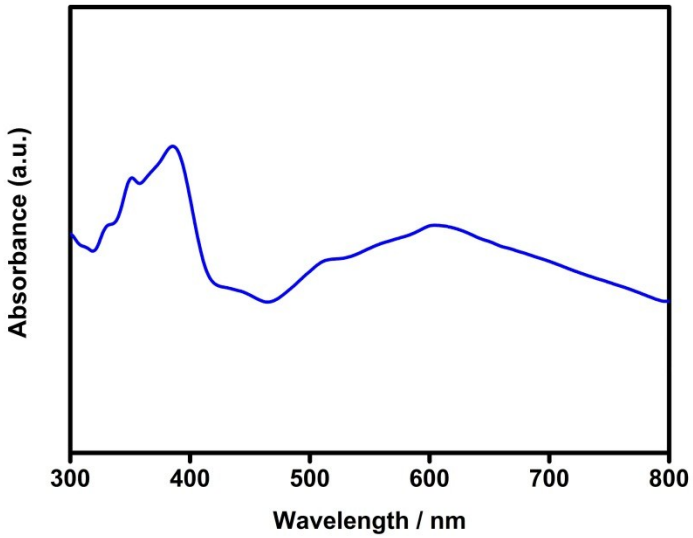

Fig. S4 Solid-state UV-Vis spectrum of NUPF-3.

S5. Channels in NUPF-3.

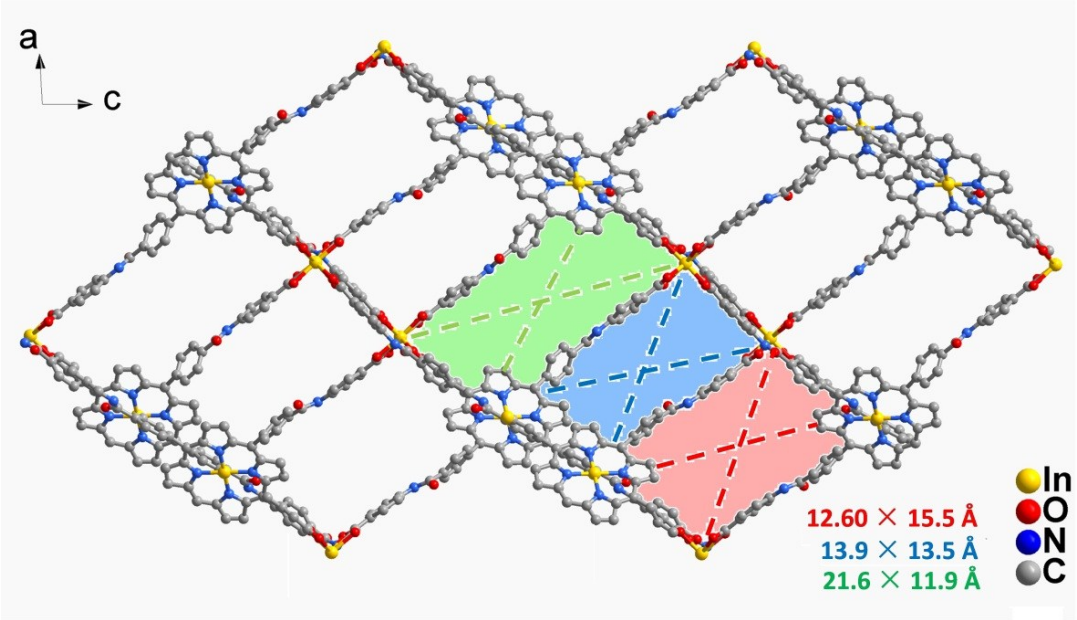

Fig. S5 Rhombic channels propagate along the *b*-axis in NUPF-3. The distances were atom to atom distances.

S6. N_2 adsorption/desorption isotherms of NUPF-3.

N_2 adsorption/desorption isotherms of NUPF-3 were measured after the sample activated by super-critical carbon dioxide (SCD). The BET surface area and pore volume determined by N_2 adsorption were 38 m^2/g and 0.018 cm^3/g, respectively. The limited N_2 adsorption of NUPF-3 indicates its very low affinity toward N_2.

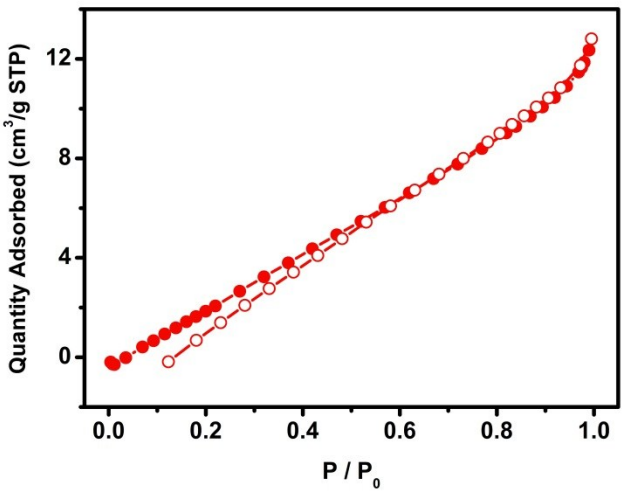

Fig. S6 N_2 adsorption/desorption isotherms of NUPF-3 measured at 77 K.

S7. Dye adsorption experiments of NUPF-3.

In order to confirm the anionic nature of NUPF-3, a dye adsorption experiment was performed. 10 mg dry NUPF-3 samples were added into 5 mL 0.12 mM methyl orange (MO) and methyl violet (MV) solutions, respectively. The mixtures were shaken via a shaker at 180 rpm for 12 hours. Results indicate that NUPF-3 has strong adsorption toward cationic MV and no adsorption of anionic MO (Fig. S7). The selective adsorption of cationic dye clearly demonstrates the anionic nature of NUPF-3.

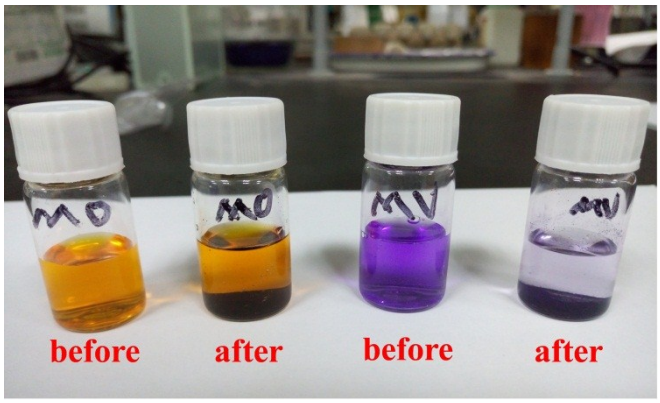

Fig. S7 Results of dye adsorption experiments of NUPF-3.

S8. Catalytic reactions.

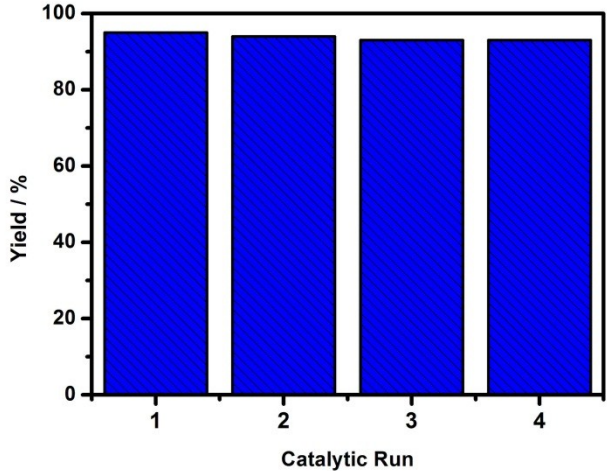

Fig. S8 Recycle experiments of NUPF-3 for the cycloaddition of CO_2 with 2-methyloxirane.

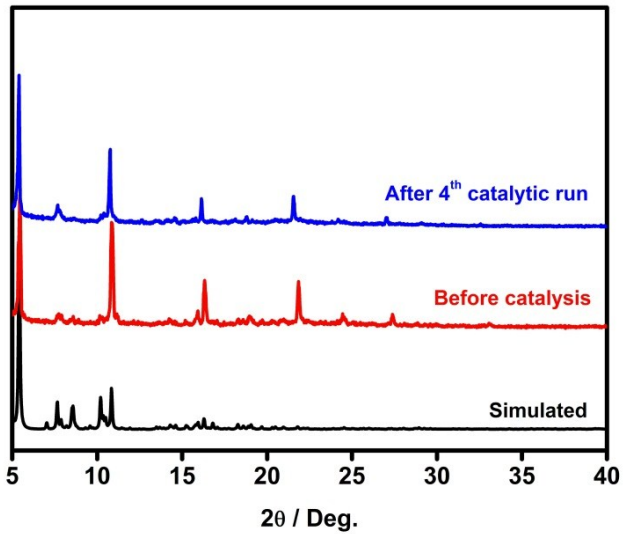

Fig. S9 PXRD patterns of NUPF-3 before and after 4th catalytic run.

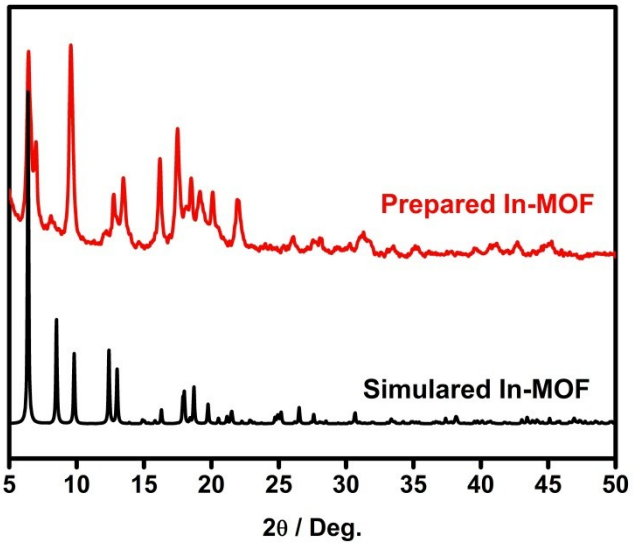

Fig. S10 PXRD patterns of In-MOF simulated and as-synthesized.

^{1}H NMR characterization data:

4-Methyl-1.3-dioxolan-2-one: colorless oil. ^{1}H NMR ($CDCl_3$, 300 MHz) δ 1.45 (d, 3H), 3.95-3.99 (m, 1H), 4.50-4.56 (m, 1H), 4.79-4.87 (m, 1H).

4-Chloromethyl-1,3-dioxolan-2-one: colorless oil. ^{1}H NMR ($CDCl_3$, 300 MHz) δ 3.65-3.80 (m, 2H), 4.35 (dd, 1H), 4.54 (t, 1H), 4.69-5.0 (m, 1H).

Tetrahydro-4H-cyclopenta[d][1,3]dioxol-2-one: colorless oil. ^{1}H NMR ($CDCl_3$, 300 MHz) δ 1.61-1.80 (m, 4H), 2.03-2.08 (m, 2H), 5.10 (m, 2H).

4-Phenyl-1,3-dioxolan-2-one: white solid. ^{1}H NMR ($CDCl_3$, 300 MHz) δ 4.21 (t, 1H), 4.65 (t, 1H), 5.60 (t, 1H), 7.25-7.30 (m, 2H), 7.26-7.31 (m, 3H).

4-Ethyl-1,3-dioxolan-2-one: white solid. ^{1}H NMR ($CDCl_3$, 300 MHz) δ 0.96 (t, 3H), 1.72 (m, 2H), 4.08 (m, 1H), 4.48-4.55 (m, 1H), 4.60-4.70 (m, 1H).

4-n-Butyl-1,3-dioxolan-2-one: yellow oil. ^{1}H NMR ($CDCl_3$, 300 MHz) δ 0.87 (t, 3H), 1.31-1.38 (m, 4H), 1.63-1.73 (m, 2H), 3.39-4.05 (m, 1H), 4.47-4.53 (m, 1H) 4.65-4.70 (m, 1H).

4-((Allyloxy)methyl)-1,3-dioxiolan-2-one: colorless oil. ^{1}H NMR ($CDCl_3$, 300 MHz) δ 3.62-3.78 (m, 2H), 4.07 (m, 2H), 4.39-4.45 (m, 1H), 4.53-4.55 (m, 1H), 4.88 (m, 1H), 5.21 -5.32 (m, 2H), 5.84-5.95 (m, 1H).

S9. Table S1 Crystal data for NUPF-3.

Compound	NUPF-3
CCDC number	1491888
Empirical formula	$C_{80}H_{55}In_2N_9O_{19.5}$
Formula weight	1683.97
Temperature	153 K
Wavelength	0.71073 Å
Crystal system	Monoclinic
space group	$P2_1/c$
Unit cell dimensions	a=21.038(3) Å α = 90 °
	b=12.5112(17) Å β = 94.509(4) °
	c=53.184(7) Å γ= 90 °
Volume	13955(3) Å^3
Z, Calculated density	4, 0.802 mg/m^3
Absorption coefficient	0.373 mm^{-1}
F(000)	3408
Theta range for data collection	2.032 to 25.682 °
Reflections collected / unique	90761 / 26224 [Rint = 0.0783]
Completeness to theta = 27.64	98.9 %
Absorption correction	Semi-empirical from equivalents
Refinement method	Full-matrix least-squares on F^2
Data / restraints / parameters	26224/1066/1093
Goodness-of-fit on F^2	1.134
Final R indices [I>2sigma(I)]	R1 = 0.1458, wR2 = 0.3665
R indices (all data)	R1 = 0.1696, wR2 = 0.3665
Largest diff. peak and hole	2.17/-3.77 e.A^{-3}

S10. References.

[1] V. A. Blatov, A. P. Shevchenko, D. M. Proserpio, *Crystal Growth & Design* **2014**, *14*, 3576-3586.